Implementing silica aerogel particles in textile reinforced cement (TRC) composites: effect of using 2D vs. 3D textile reinforcement

Zochiou, Lamprini; Snels, Laurens; Seveno, David; Tysmans, Tine; Triantafillou, Thanasis

Publication date:
2025

Document Version:
Accepted author manuscript

IMPLEMENTING SILICA AEROGEL PARTICLES IN TEXTILE REINFORCED CEMENT (TRC) COMPOSITES: EFFECT OF 2D VS. 3D TEXTILE REINFORCEMENT

Lamprini Zochiou[1,2*], Laurens Snels[3], David Seveno[3], Tine Tysmans[1], Thanasis Triantafillou[2]

[1] Department of Mechanics of Materials and Constructions, Vrije Universiteit Brussel, 1050 Brussels, Belgium; Tine.Tysmans@vub.be

[2] Department of Civil Engineering, Structural Materials Laboratory, University of Patras, 26504 Rio, Greece; ttriant@upatras.gr

[3]Department of Materials Engineering, KU Leuven, 3001 Leuven, Belgium; laurens.snels@kuleuven.be, david.seveno@kuleuven.be

** Correspondence: Lamprini.Zochiou@vub.be*

SUMMARY:

In this study, the incorporation of super-insulating silica aerogel particles in textile reinforced cement (TRC) composites is investigated, to obtain a lightweight material that combines adequate mechanical properties and significant thermal conductivity. The inclusion of hydrophobic aerogel particles into a cementitious matrix – further referred to as 'aerocement' – inevitably leads to a drop in the mechanical performance, considering the lower density of the composite and the lack of bonding between cement and aerogel particles as major factors. This effect was quantified by three-point bending and compression tests on mortar prisms. The current study then focuses on the mechanical properties of aerocement reinforced with two- or three-dimensional basalt or glass textile. Each series was characterized by four-point bending tests in terms of mechanical properties and composite behavior. While the fiber type (basalt, glass) did not significantly affect the composites response, the transversal connections in the 3D textiles did improve the strength and crack formation more, compared to the 2D-reinforced aerocement composites.

KEY WORDS:

aerogel particles, cement composites, mechanical properties, lightweight concrete, textile reinforced cement

1. INTRODUCTION

As noted by the European Commission statistics, collectively, buildings in Europe are responsible for 40% of energy consumption and 36% of greenhouse gas emissions [26]. The energy efficiency, which is among the highest current needs in construction, is highly linked to the insulation that the building shell can provide and to the materials used. The most common construction materials such as concrete or masonry do not fulfill this requirement unless they are combined with additional layers of external insulation systems, which inevitably leads to an increased total building shell thickness. For this reason, novel materials combining low thermal conductivity and low density, with high compressive strength could be promising for building applications and should be investigated [19, 26].

The present paper, therefore investigates the incorporation of silica aerogel particles into a cement mix. Silica aerogel is a nanoporous material with a very high specific surface and an extremely high porosity up to 99.8%, with typical values at least equal to 95% [21, 28, 30]. It is extremely lightweight and provides the lowest thermal conductivity of all existing solids, of around 0.014 W/mK, which makes it, among other applications, perfect for thermal and acoustic insulation purposes [28]. Silica aerogel was

found in the 1930s but only the last twenty years have brought considerable interest in this material [1], with the development of aerogel concrete starting in 2008 [27]. In this first study, superhydrophobic aerogel particles were added in volumes between 50% and 70% to CEMI and CEMII cement mixtures. The produced specimens showed excellent properties such as low thermal conductivity, high sound absorption and high fire resistance. However, a low Young's Modulus and a very low compressive strength were obtained [29]. The drop in mechanical performance of the aerogel-incorporated cement is inevitable, considering the lower mechanical strength and density of the aerogel particles compared to a pure cement mix and the high volume of the aerogel in the mix. By investigating though the percentage of aerogel in the mix, the granule size and the mix design itself, it is possible to develop a light-weight, low density, super-insulating cement with adequate strength for construction purposes [14, 20, 23, 34].

The mechanical properties of an aerogel-incorporated cement may also be enhanced by reinforcing the brittle material with fiber textiles and this will be explored in the present study. In Textile Reinforced Cement (TRC) composites, the cementitious matrix provides the structural integrity and the compressive strength, however, due to its weak tensile performance, cracks will form. The role of the textile is to bridge the cracks and provide the tensile load bearing capacity of the composite. Regarding the textile's geometry, most studies in the past have dealt with two-dimensional (2D) textiles that contain reinforcing yarns only in the planar directions (X,Y). In 3D textiles, however, two planar textiles are kept in a fixed distance by transversal fiber connections [18], which provide structural integrity and a fixed lever arm inside the cross-section. The presence of reinforcement in all three directions has been found to improve the mechanical properties of the cement-based composites by eliminating brittle failure modes such as delamination and through thickness failure.

In this study, 3D-woven basalt and Alkali Resistant (AR) glass textiles were used; both are considered to be suitable for various applications including high energy absorption, low crack propagation and high tensile strength [31]. Their performance was compared with equivalently reinforced TRC elements with woven basalt and glass 2D textiles. Glass fibers, present high mechanical strength at a relatively low cost. When exposed to highly alkaline environment, natural glass fibers deteriorate, so for cement applications AR glass fibers are used to ensure durability into the cementitious matrix [4, 24]. Basalt fibers come with higher mechanical properties, especially in terms of tensile strength, as well as a production of lower cost and energy consumption [9], together with high resistance to alkalis and a wide range of thermal performance, which is of great interest considering the combination with a super-insulative matrix.

2. MATERIALS AND METHODS

2.1. Materials

In this study, superhydrophobic aerogel particles were used (P100, Cabot, Germany), with a particle size of 0.1-4.0 mm and a thermal conductivity of ≤ 0.02 W/(mK). They have a porosity higher than 90%, a bulk density of 80-100 kg/m^3 and a specific area of 600-800 m^2/g [8]. The aerogel particles were added to a cementitious matrix composed of Portland cement (CEM I 52.2 N, Holcim, Belgium), tap water and superplasticizer (Melflux 4930F, BASF, Germany). The particle size distribution of the aerogel was chosen to be close to a regular fine sand, so to fill in its role, in a mix with no presence of sand or any other coarse aggregates since, according to literature, in that case aerogel fracture during mixing will be increased [16]. A low water-to-cement ratio was chosen, attempting to keep the compressive strength at high levels, provided that the workability of the fresh mortar is still adequate. Superplasticizer was added to obtain a well-mixed and flowable paste. The mix (Table 1) was designed by the second author of this study in the framework of the collaborative research project 'Aerocon' (see acknowledgements).

Table 1. *Mix Design of 'aerocement': amounts given for one TRC specimen (500x60x17 mm^3).*

Aerocement mix	Cement (g)	Water (g) w/c = 0.33 p.w.	SP (g) SP/c = 0.002 p.w.	Aerogel (g) a/c = 0.07 p.w.
	464.84	153.40	0.93	32.54

The textiles used as reinforcement were orthogonally woven, two- and three-dimensional, made of basalt or glass (3D Weaving, Belgium) [3]. A typical Leno weave was used, with a polyester filament in the warp direction to keep the fibers in place, as well as in the through-thickness direction for the three-dimensional textile to ensure their inter-layer distance. The mesh geometry and properties of the textiles

are given in Table 2. To determine the mechanical properties of the basalt and glass fiber bundles tensile tests were performed at both a yarn and textile level [33]. In the case of specimens reinforced with two-dimensional textiles, two identical layers were stitched together and placed at the top and bottom of the specimen. In the case of three-dimensional textiles, one 3D textile was combined with two additional single layers of textile, one on its top and one on its bottom. The configurations, shown in Fig. 2c-d, were identical for both glass and basalt textiles, at all cases ensuring the same fiber volume fraction of 1%, higher than the critical volume fraction to obtain a strain-hardening behavior after matrix cracking [32].

Table 2. *Properties of woven, basalt and glass, 2D and 3D textiles [33].*

Material	2D Basalt	3D Basalt	2D Glass	3D Glass
Mesh size (mm)	9.1 x 9.1	(weft) 9.1 x 9.1 (warp) 7.5 x 7.5 & 15.1 x 15.1 at transversal connectors	9.1 x 9.1	(weft) 9.1 x 9.1 (warp) 7.5 x 7.5 & 15.1 x 15.1 at transversal connectors
Linear Density (tex)	1200	2 layers of 1200 each	1200	2 layers of 1200 each
Inter-layer distance (mm)	-	8.5	-	8.5
Fibers tensile strength (MPa)	2800	2800	1900	1900
Specific gravity (g/cm^3)	2.69	2.69	2.68	2.68
Transversal and planar connectors' material	Polyester PET	Polyester PET	Polyester PET	Polyester PET

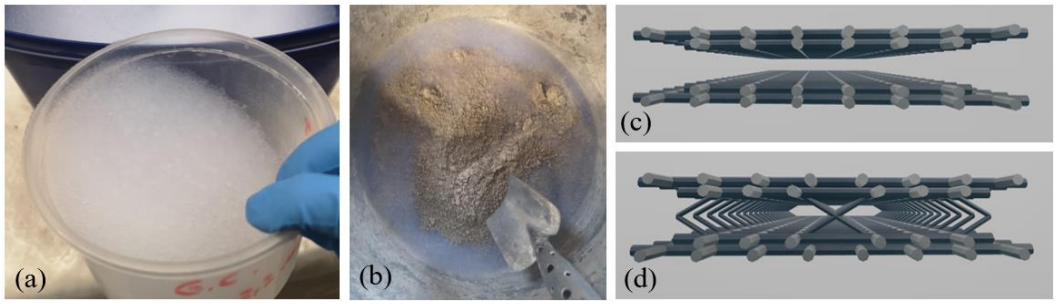

Figure 2. (a) *P100 silica aerogel particles (b) aerogel particles and cement before mixing (c) textile 2L-2D+2L-2D (d) textile 1L-3D+2L-2D.*

2.2. Preparation of specimens

2.2.1 Preparation of prism specimens

Before investigating TRC specimens, the mechanical performance of the aerocement was characterized. For this purpose, prismatic specimens were prepared, using steel moulds of 40x40x160 mm^3.

Considering the lightweight and hydrophobic nature of the aerogel, first the cement powder and the aerogel particles were dry mixed for 30 seconds at low speed of 140 rpm (Fig. 2b). The superplasticizer was dissolved into water to create an activated solution that was then added to the dry mix, while mixing at low speed of 140 rpm for 60 seconds, to create a well-mixed and flowable paste where all aerogel particles were covered and incorporated into the cementitious slurry. The mixing has to be as low-speed and short as possible to minimize the inevitable fracture of some of the largest particles. The moulds were filled in two layers, and after each layer modest vibration generated by a vibrating table was applied for a less than 10 seconds, to avoid segregation of the aerogel particles, considering its lightweight nature.

The top of the moulds was then covered with a plastic sheet to avoid water evaporation, and the specimens were left to harden for three days at room temperature. After demoulding, the prisms were weighed and wrapped in plastic foil and left to cure at a constant temperature of 20°C until tested at an age of 28 days.

2.2.2 Preparation of TRC specimens

For the manufacturing of the TRC specimens, moulds of 500x60x17 mm^3 were used with various parts made of hardened plastic and steel, in accordance with RILEM recommendations [6]. These custom-

made moulds ensure the position of the top and bottom layer of the textile and a uniform cover thickness of 2 mm on both sides of the specimen, by a built-in clamping system [17]. For each layer of reinforcement where two textiles are stitched together (Fig. 2c-d), one of them is cut precisely to the dimensions of the mould and the other one is cut longer in width, to be clamped between the mould's top and bottom parts. For all configurations, there are six yarns actively working in the cross section in the direction of the load, and two additional yarns, one on each side, that are left for the textile to be clamped, as shown in Fig. 3.

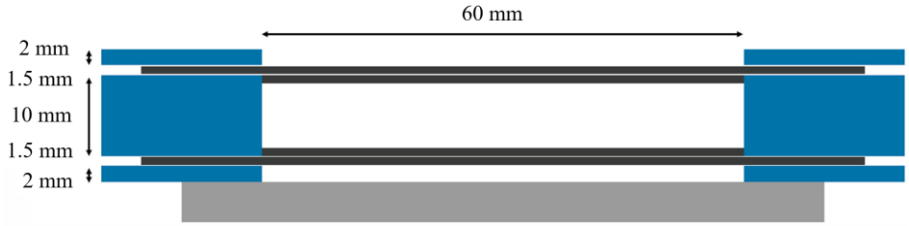

Figure 3. *Cross-section of custom-made TRC mould [33].*

Once the textiles were secured in place, the aerocement matrix was prepared as described in §2.2.1, and poured into the moulds. During the pouring process, gentle vibration was applied, to enhance the passing of the matrix through all the layers of the textile. The moulds were filled in two layers and after the completion of each one, vibration was modestly increased, but always kept at less than 10 seconds in time, to avoid separation of the mix and concentration of the aerogel particles at the top of the specimen.

The top of the moulds was then covered with a plastic sheet to avoid surface evaporation, and the specimens were left to harden for at least three days, as earlier demoulding could cause breaking of the specimens and severe scratching of their top surface. After demoulding, their actual thickness was measured, they were wrapped in plastic foil and left to cure at a constant temperature of 20°C until tested at an age of 28 days.

2.3. Methods

2.3.1 Characterization of aerocement mix

Adding aerogel particles into a 52.5N cement mix can highly affect the flowability, which is of high importance since the mix should be pourable to cast through 3D textile reinforcement. The flowability of the mix was therefore measured using a flow table, following the procedure defined in EN 12350-5 [11].

The mechanical strength in bending and compression of the aerocement matrix was determined by means of three point bending tests on prisms of 40x40x160 mm^3 and compression tests on the halves, both according to the EN 12390, part 5 [13] and part 3 [12] respectively. A universal Instron 5982 test bench was used, with a load cell of 5 kN for the bending test and 100 kN for the compression test, and a constant loading rate of 0.5 mm/min (displacement control). The set-up can be seen in Fig. 4a-b.

2.3.2 Characterization of TRC specimens

For the TRC specimens, their mechanical response was evaluated by means of four-point bending tests on an Instron 5982 test bench with a load cell of 5 kN and a constant loading ratio of 2 mm/min (displacement control). The steel supports of the set-up have a distance of 350 mm, and the loading pins have a distance of 100 mm from each other. To more precisely monitor the displacements and the crack initiation and propagation during the test, Digital Image Correlation (DIC) was used, with two sets of two cameras with a pixel density of 2448 by 2048 pixels, a first set of two monitoring the bottom surface of the specimen parallel to textile plane and the other two the side surface. The DIC acquisition rate was every 10 N or every 4 seconds.

The software Vic-3D 10, from Correlated Solutions, was then used to analyze the captured images, using a subset size of 21 for the side of the TRC and 43 for the bottom, a step size of 7 or 13 respectively, and a strain window of 9. For all DIC monitoring of the sides of the samples, the extracted data are the vertical displacements of the speckle patterns and for DIC monitoring the bottom was the crack formation. The four-point bending test set-up can be seen in Fig.4c.

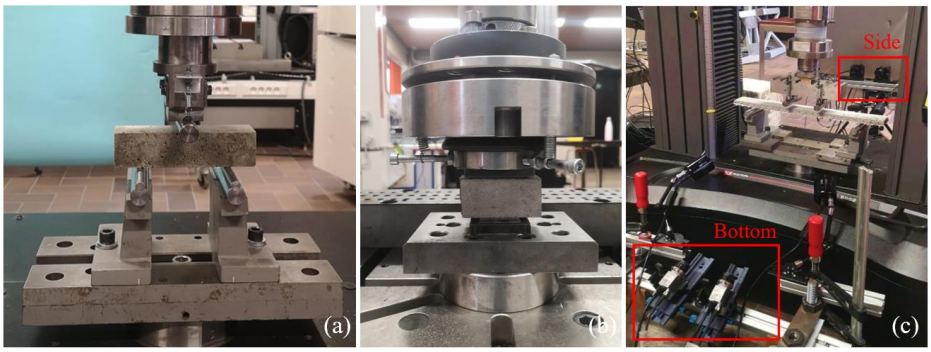

Figure 4. *Test set-up: (a) three-point bending (b) compression (c) four-point bending-DIC.*

3. RESULTS AND DISCUSSION

3.1 Mechanical Properties of 'aerocement' matrix

The 'aerocement' mix, used as the matrix for the textile reinforced cement specimens, contains aerogel particles at a percentage of 50% per volume. By replacing at a high percentage normal aggregates such as sand or other coarse aggregates in a cement mix, with such a light-weight solid having a density of 100 kg/m^3, a light-weight cement is obtained. The main properties of the mix are presented in Table 3.

Table 3. *Properties of the 'aerocement' matrix.*

	Flowability (cm)	Density after demoulding (kg/m^3)	Compressive strength (28d) (MPa)	Bending strength (28d) (MPa)
Aerocement mix	24.5	1259.5 ± 96.9	13.5 ± 2.7	2.8 ± 0.4

An important prerequisite of the mix was the adequate flowability in order for it to be pourable during casting and to ensure passing through the textile spacings. The flowability of the fresh paste, the hydration process of the mix and the long-term mechanical properties of the mortar are very sensitive to the mixing process, due to the interface interaction of the aerogel particles with cement and water, thus the mixing process described in §2.2.1 was followed precisely.

Figure 5. *Aerocement prism cross-section cut.*

Following the tests, the internal cross section of the prisms was observed, to evaluate the presence and homogeneous distribution of the aerogel particles inside the mix (Fig. 5). They were found to be homogeneously distributed throughout the cross section without noticing local cement concentrations. The theoretically calculated density according to the mix design is 1040 kg/m^3, comparable to the experimentally measured density considering the average value and the standard deviation (Table 3), so the inevitable breaking of larger particles during the mixing process remained within acceptable levels.

3.2 Four-point bending tests on textile reinforced aerocement

3.2.1 Mechanical behavior

The results of the four-point bending tests on textile reinforced aerocement specimens are presented below. Fig. 6 shows the load vs. displacement curves obtained from the mechanical loading of the specimens and Table 4 summarizes the average values together with the standard deviations of the main mechanical properties, namely the first cracking and the ultimate load as well as the flexural stiffnesses in the pre- and post-cracking stages.

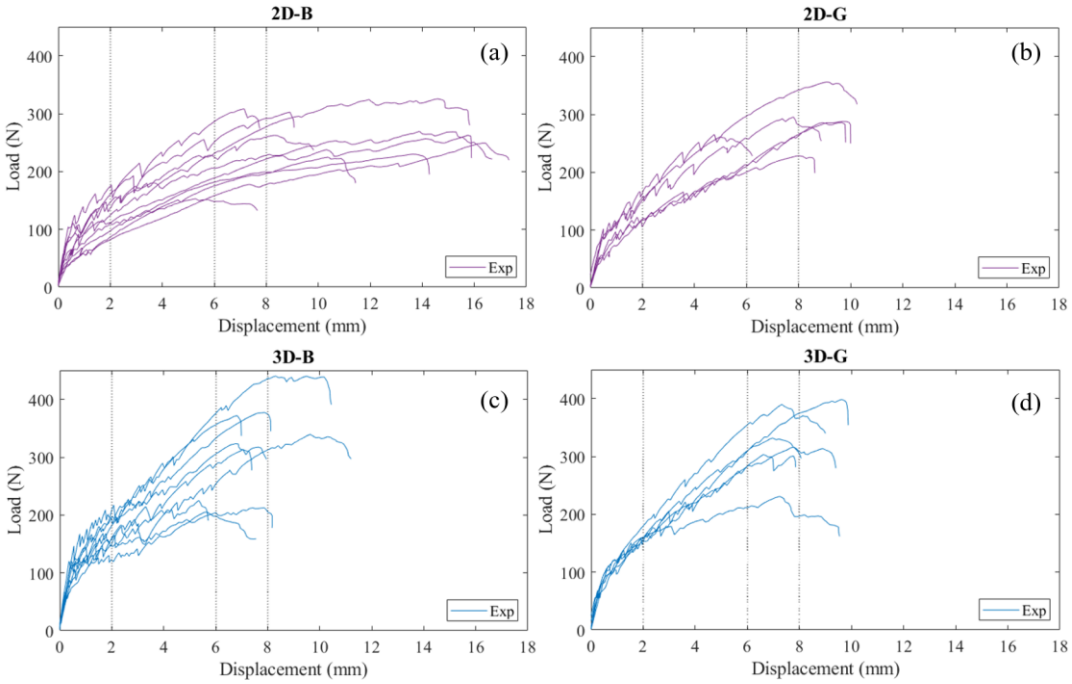

Figure 6. *Load vs. displacement curves from four-point bending tests: (a) 2D-basalt textile (b) 2D-glass textile, (c) 3D-basalt textile (d) 3D-glass textile.*

Table 4. *Mechanical properties obtained from TRC four-point bending tests.*

Specimen's ID	Cracking Load (N)	Failure Load (N)	Pre-Cracking Stiffness (N/mm)	Post-Cracking Stiffness (N/mm)
2D-B	79.7 ± 19.8	258.3 ± 47.2	131.5 ± 60.9	18.0 ± 5.7
3D-B	121.3 ± 17.8	321.4 ± 77.6	208.2 ± 75.3	28.7 ± 8.2
2D-G	98.4 ± 3.6	274.2 ± 25.1	134.7 ± 45.3	24.3 ± 8.2
3D-G	109.9 ± 37.1	328.4 ± 38.9	197.8 ± 71.2	36.7 ± 6.0

Even though there is a wide range in the response of most groups of specimens, trends and main characteristics, can be clearly discussed and compared. The typical TRC response in bending, consists of three stages, as described by the ACK theory: an initial stage where the TRC composites behave linearly elastic until the formation of the first crack in the matrix, the second stage with further microcracking in the matrix and redistribution of stresses to the textile, and the third stage with crack widening and no significant new crack formation until failure [2]. Therefore, the pre-cracking flexural stiffness is calculated between the beginning of loading and the first cracking load. Considering that the tested TRC specimens do not form a very distinct micro-cracking phase and post-cracking behavior, the post-cracking stiffness is calculated between the first cracking load and the ultimate load.

For the 2D-TRCs with basalt textile, there is no distinct micro-cracking and post-cracking phase. After the initiation of cracking in the matrix, the cracks increased continuously in both number and width until the specimens reached the ultimate load. The failure mode was crushing of cement at the top of the specimen, either in the middle of the compression zone (Fig.7a) or under the loading pins (Fig.7c).

For the 3D-B group, a post-cracking stage was more noticeable with an increase in stiffness after the micro-cracking phase and until the ultimate load, showing increasing crack width and no significant new crack formation. Both the cracking load and the failure load correspond to higher values compared to 2D-B series but occurred in lower displacements, considering the average value and the standard deviation for all amounts (Table 4). This is highly linked to the higher values of pre-cracking and post-cracking stiffnesses that were derived from the graphs of the specimens with the 3D transversally connected textile compared to the equivalent 2D alternative. Two different failure modes were observed for the 3D-B group: for the majority of specimens it was due to tensile failure of the bottom reinforcement (Fig.7d) and for a minority, due to cement crushing in the middle of the compression zone (Fig.7a)

The 2D-G group of specimens, reinforced with two-dimensional woven glass textile, performed in a way similar to the equivalently reinforced 2D-B group. The cracking initiation in the matrix and the failure occurred for comparable load levels. However, compared to their equivalents, the results from the 2D-G group of specimens were more consistent and it was possible to differentiate between the micro-cracking and the post-cracking phase, approaching in a closer way the typical TRC behavior. Two types of failure modes were again observed: the tensile failure of the bottom reinforcement (Fig.7d) and the crushing of the top cement layer under one of the loading pins (Fig.7).

3D-G series, also behaved in a similar way as the equivalent series of specimens 3D-B, reinforced with the 3D woven basalt textile, outperforming the response of the 2D-reinforced specimens. When considering the load and stiffness values of interest, as happened for the 2D-G, again the range is not very wide. When attempting for a qualitative approach though, it can be seen that for some specimens a strain-hardening behavior arose, whereas for the rest, although it is still possible to differentiate between the microcracking and post-cracking phase, the formation of new cracks with increasing load was quite important until their failure. For this group of specimens, failure occurred through two different modes: tensile failure of the bottom reinforcement (Fig.7d) followed by spalling of the cement at the tensile zone for some specimens (Fig.7b) or crushing of cement in the middle of the compression zone (Fig.7a).

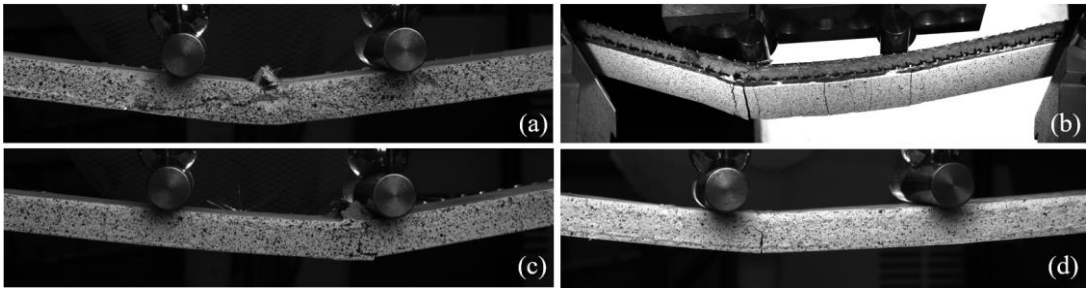

Figure 7. *Failure mechanisms observed: (a) aerocement crushing at the middle of the compression zone (b) bottom aerocement spalling (c) aerocement crushing under loading pin (d) tensile failure.*

3.2.2 Crack formation

Apart from the mechanical properties of the tested specimens, the crack formation was also investigated by means of DIC, monitoring their bottom side parallel to the textile plane (Fig. 8b). Due to the range of the results, it was decided to monitor the crack pattern for three different values of midspan displacement: at 2 mm, which corresponds to early stages of the crack formation, at 6 mm which mostly corresponds to middle or later stages of the cracking phase and at 8 mm, which is right before or right after the specimen's failure. The selected displacements are indicated in the load-displacement graphs (Fig. 6).

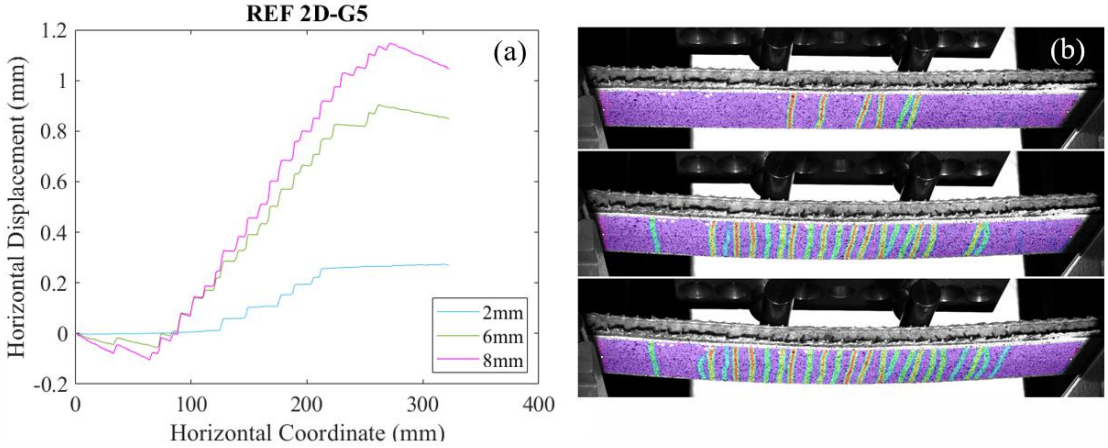

Figure 8. (a) *Crack visualization along a spanning line for sample 2D-G5 (b) crack visualization by DIC 'strain fields' for sample 2D-G5, at displacement of 2, 6 and 8 mm.*

The number of cracks and the crack width were investigated by creating a horizontal line, spanning the length of the specimen between the supports and then by plotting the relative horizontal displacement of different points on that line (Fig. 8a). Every jump marks the formation of a new crack, where the vertical dimension of the jump is equal to the crack width and the horizontal to the gap between adjacent cracks.

In Fig. 8b a representation of the cracks can be seen for a selected TRC specimen, reinforced with 2D glass textile. It is important to note that the DIC strain fields used, are only a way to visualize the crack formation and not an actual strain concentration as no material is present in the crack area [10]. DIC measures the relative displacement of the points of the speckle pattern, so, for example, the areas with red-shaded colors represent a larger relative displacement corresponding to a crack. An efficient TRC cross-section would provide sufficient load redistribution between the matrix and the textile reinforcement, so a high number of cracks with small crack width should be expected to form [33].

Table 5 presents the average values together with the standard deviations, of the number of cracks that formed, as well as the crack width and distance, for all three levels of measured displacements.

Table 5. *Crack parameters obtained from TRC four-point bending tests.*

Specimen's ID	Displacement (mm)	Number of cracks	Crack width (μm)	Crack distance (mm)
2D-B	2	9.9 ± 3.6	40.3 ± 15.9	14.6 ± 5.1
	6	15.9 ± 5.1	69.1 ± 29.6	9.6 ± 3.8
	8	17.2 ± 5.5	94.2 ± 33.2	8.9 ± 3.5
3D-B	2	8.9 ± 1.9	42.4 ± 13.1	16.3 ± 5.7
	6	21.0 ± 2.5	56.7 ± 11.9	5.2 ± 0.5
	8	22.6 ± 2.3	59.5 ± 10.6	4.4 ± 0.6
2D-G	2	7.5 ± 1.5	39.5 ± 4.9	17.6 ± 4.8
	6	15.8 ± 3.4	68.8 ± 16.1	10.3 ± 2.7
	8	17.8 ± 4.2	79.3 ± 22.7	8.7 ± 2.9
3D-B	2	10.2 ± 3.8	30.9 ± 5.7	11.8 ± 2.4
	6	20.5 ± 7.5	48.3 ± 4.7	6.7 ± 1.0
	8	25.2 ± 1.6	58.9 ± 3.3	5.9 ± 1.6

For the 2D-reinforced specimens, both with basalt and glass textiles, fewer cracks with larger openings were observed in all measured displacements and the crack propagation manifested itself with increasing crack width rather than formation of new cracks. On the contrary, the 3D-reinforced specimens permitted the formation of steadily higher amounts of cracks in all loading stages, with smaller crack width and smaller distances between adjacent cracks, compared to their 2D-reinforced counterparts (Table 5). For measured displacements from 2 to 6 mm, which correspond to the micro-cracking phase for all groups of specimens, the number of cracks was double or higher for the 3D-TRCs series and the crack width kept increasing. From 6 to 8 mm which is already well in the post-cracking phase, the crack formation is more stabilized with fewer new cracks and controlled widening of the existing ones. Therefore, this can be an indication, together with what was discussed in §3.2.1, that the transversal fiber connections enable a more efficient combined performance and redistribution of forces between the aerocement matrix and the textile.

4. CONCLUSIONS

In this study, the incorporation of silica aerogel particles into a cement mix that can be used as the matrix in textile reinforced cement (TRC) composites was explored. The 'aerocement' was firstly characterized in bending and compression and the challenges that may arise due to the porous and light-weight nature of the aerogel particles were investigated and discussed. The matrix was combined with uncoated, woven, basalt and glass, 2D and 3D textile reinforcement and the specimens were tested in four-point bending.

The results for all groups showed a quite wide range, however it can be concluded that the combination of aerocement with textiles provides a promising development of a light-weight, insulative element with considerable strength. When aerocement was used as a matrix, a combined action between the matrix and the fibers that approaches the ACK theory arose, with formation of microcracking and redistribution of forces to the fibers during loading. The choice of fiber type (glass or basalt) for the textile reinforcement

had no significant effect on the performance. The post-cracking stage was more clearly observed for the 3D-reinforced specimens for both materials rather than for their 2D counterparts, showing that indeed the transversal fiber connections present in the 3D textile beneficially affect the bending behavior of a TRC composite. For the 3D-TRCs, failure occurred at higher levels of load and relatively smaller values of displacements, again showing the increase in stiffness that the 3D textile architecture can provide.

This finding can be linked to the microstructure of 'aerocement'. When its porous bulk is enclosed between the two layers of the textile, shear phenomena are more controlled and redistribution of stresses is more likely through the connectors, guiding towards a strain-hardening tensile behavior and less brittle failure modes. However, due to the lower mechanical properties of the aerocement matrix compared to a conventional cement mix (Table 3), and the presence of aerogel in the thin faces (2 mm) of the TRC coupons, brittle mechanisms, namely cement crushing in the middle of the compression zone or under the loading pins could not be avoided for an important number of tested specimens.

Therefore, this leads the research towards further investigation of the mechanical properties of the aerocement matrix, regarding the mix design itself and the interaction of the hydrophobic aerogel particles with the rest of the precursors in the mix. Thermal conductivity tests will determine the level of the aerogel content in the mix, to effectively exploit the super-insulative and fire-protection potential of aerogel without counteracting the mechanical properties of the matrix and as a result, of the composite element. Future work will also explore different casting techniques and configurations for the TRC coupons to more efficiently reinforce the aerocement matrix towards eliminating brittle mechanisms.

Acknowledgements

This research is funded by the Research Foundation-Flanders (FWO Vlanderen) as part of an SBO project, "A new generation of high performance building materials and elements integrating aerogels and textile reinforced cement composites" (S008023N).

5. REFERENCES

[1]AEGERTER M. A., LEVENTIS N., KOEBEL M. M., "Aerogels Handbook", *Advances in Sol-Gel Derived Materials and Technologies*, 2011.

[2]AVESTON J., COOPER G.A., KELLY A., "Single and multiple fracture", *Properties of Fibre Composites*, 1971, p. 15-26.

[3]Basaltex, *Technical Data Sheet Basalt roving*, Wevelgem, 2022.

[4]BENTUR A., BEN-BASSAT M., SCHNEIDER D., "Durability of Glass-Fiber-Reinforced Cement with Different Alkali-Resistant Glass Fibers", *Journal of the American Ceramic Society*, vol. 68, n ° 4, 2006, p. 203-208.

[5]BENTUR A., MINDESS S., *Fibre reinforced cementitious composites*, Editions Taylor & Francis Group, 2007.

[6]BRAMESHUBER W., "Recommendation of RILEM TC 232-TDT: test methods and design of textile reinforced concrete", *Materials and Structures*, vol. 49, n ° 12, 2016, p. 4923-4927.

[7]BRAMESHUBER W., *Textile Reinforced Concrete: State of the Art Report*, RILEM Technical Committee, RILEM Publications, 2006.

[8]CABOT, *Technical Data Sheet Aerogel P100-P300*, Germany, 2021.

[9]DEAK T., CZIGANY T., "Chemical Composition and Mechanical Properties of Basalt and Glass Fibers: A Comparison", *Textile Research Journal*, vol. 79, n ° 7, 2009, p. 645-651.

[10]EL KADI M., TYSMANS T., VERBRUGGEN S. et al, "Experimental study and benchmarking of 3D textile reinforced cement composites", *Cement and Concrete Composites*, vol. 104, 2019.

[11] EN 12350-5:2019, *Testing fresh concrete - Part 5: Flow table test*, 2019.

[12] EN 12390-3:2019, *Testing hardened concrete - Part 3: Compressive strength of test specimens*, 2019.

[13] EN 12390-5:2019, *Testing hardened concrete - Part 5: Flexural strength of test specimens*, 2019.

[14]FICKLER S., MILOW B., RATKE L. et al., "Development of high performance aerogel concrete", *Energy Procedia, 2015*, p. 406-411.

[15]FIORE V., SCALICI T., DI BELLA G., VALENZA A., "A review on basalt fibre and its composites", *Composites Part B: Engineering*, vol. 74, 2015, p. 74-94.

[16]GAO T., JELLE B., GUSTAVSEN A., JACOBSEN S., "Aerogel-incorporated concrete: An experimental study", *Construction and Building Materials*, vol. 52, 2014, p. 130-136.

[17]GIELIS C., EL KADI M., SNOECK D., TYSMANS T., "3D Textile Reinforced Cement (TRC) composites with integrated synthetic microfibres: Evaluation of mechanical response and crack formation in bending", *Construction and Building Materials*, vol. 426, 2024.

[18]HAIK R., ADIEL S. E., PELED A., "Influence of three-dimensional (3D) fabric orientation on flexural properties of cement-based composites", *Cement and Concrete Composites*, vol. 80, 2017, p. 1-9.

[19]KOLOKOTSA D., ROVAS D., KOSMATOPOULOS E., KALAITZAKIS K., J.," A roadmap towards intelligent net zero- and positive-energy buildings ", *Solar Energy*, vol. 85, n ° 12, 2011, p. 765-795.

[20]LI P., WU H., LIU Y. et al., "Preparation and optimization of ultra-light and thermal insulative aerogel foam concrete", *Construction and Building Materials*, vol. 205, 2024, p. 529-542.

[21]LIU Z. H., WANG F., DENG Z. P., "Thermal insulation material based on SiO2 aerogel", *Construction and Building Materials*, vol. 122, 2016, p. 548-555.

[22]NAAMAN A. E., SCHNELLENBACH H. M., WELSCH T., "Textile reinforced cement composites: competitive status and research directions", *Conference in Material Science*, Aachen, *RILEM publications*, 2010, p. 3-22.

[23]NG S, JELLE B., SANDBERG L. et al., "Experimental investigations of aerogel-incorporated ultra-high performance concrete", *Construction and Building Materials*, vol. 77, 2015, p. 307-316.

[24]PAUL S., GETTU R., NAIDU A. D., SAMANTHULA R., "Experimental evaluation of the durability of glass Textile-Reinforced concrete", *Construction and Building Materials*, vol. 406, 2023.

[25]PELED A., MOBASHER B., BENTUR A., *Textile reinforced concrete*, London, Editions CRC Press, 2017.

[26]PEREZ L., ORTIZ J., POUT C., "A review on buildings energy consumption information", *Energy and Buildings*, vol. 40, n ° 3, 2008, p. 394-398.

[27]RATKE L., "Herstellung und Eigenschaften eines neuen Leichtbetons: Aerogelbeton", *Beton- und Stahlbetonbau*, vol. 103, n ° 4, 2008, p. 236-243.

[28]RIFFAT S. B., QIU G., "A review of state-of-the-art aerogel applications in buildings", *International Journal of Low-Carbon Technologies*, vol. 8, n ° 1, 2013, p. 1-6.

[29]SCHNELLENBACH H. M., WELSCH T., "Advancements in high performance aerogel concrete", *6th International Conference on Structural Engineering, Mechanics and Computation*, 2016, p. 1577-1582.

[30]SLOSARCZYK A., VASHCHUK A., KLAPISZEWSKI L., "Research Development in Silica Aerogel Incorporated Cementitious Composites—A Review", *Polymers*, vol. 14, n ° 7, 2022.

[31]TRIANTAFILLOU T., *Textile Fibre Composites in Civil Engineering*, Woodland Publishing, 2016.

[32]TYSMANS T., WASTIELS J., "Editorial on Special Issue "Textile-Reinforced Cement Composites: New Insights into Structural and Material Engineering", *Applied Sciences (Switzerland)*, vol. 10, n ° 2, 2020, p. 10-13.

[33]VANDEREECKEN G., TODERASCU C., EL KADI M., VAN HEMELRIJCK D., TYSMANS T., "Influence of coating and reinforcement volume fraction on woven basalt TRC: An experimental study", *Construction and Building Materials*, vol. 444, 2024.

[34]WELSCH T., VIEVERS Y., SCHNELLENBACH H. M., BIALUSCHEWSKI D., MILOW B., "Comparison of different aerogel granules for use as aggregate in concrete", *Gels*, vol. 9, n ° 5, 2023.